

## THE EFFECT OF MECHANICALLY ACTIVATED FLY ASH, CRYSTALLINE ADMIXTURE, AND NANO ALUMINA ON THE FRESH PROPERTIES, MECHANICAL PROPERTIES, AND SELF-HEALING OF CEMENT MORTARS

Irina Stefanovska<sup>1</sup>, Goran Markovski<sup>2</sup>, Toni Arangjelovski<sup>2</sup>, Dime Janchev<sup>1</sup>, Vojo Jovanov<sup>3</sup>, Ane Anchev<sup>4</sup>, Nikolina Stamatovska Aluloska<sup>4</sup>, Aleksandar Zlateski<sup>5</sup>, Aleksandar Zhurovski<sup>5</sup>, Emilija Fidanchevski<sup>3</sup>

<sup>1</sup>ADING AD – Skopje, Republic of North Macedonia

<sup>2</sup>Ss. Cyril and Methodius University in Skopje, Faculty of Civil Engineering, Skopje, Republic of North Macedonia

<sup>3</sup>Ss. Cyril and Methodius University in Skopje, Faculty of Technology and Metallurgy, Skopje, Republic of North Macedonia

<sup>4</sup>Cementarnica USJE-TITAN Group, Republic of North Macedonia

<sup>5</sup>Ss. Cyril and Methodius University in Skopje, Institute of Earthquake Engineering and Engineering Seismology, Republic of North Macedonia

e-mail: vojo@tmf.ukim.edu.mk

Reducing the carbon dioxide (CO<sub>2</sub>) footprint in the construction industry is a key global objective in the pursuit of sustainability, especially considering that Ordinary Portland Cement (OPC) production is a significant contributor to global CO<sub>2</sub> emissions. Numerous advanced technological solutions have been explored to mitigate this impact, with one promising approach being the partial replacement of cement with supplementary cementitious materials (SCMs), aligning with the principles of a circular economy. This study aimed to develop green mortars by replacing 16 wt.% of cement with mechanically activated fly ash. In addition, the effects of the addition of 1 wt.% crystalline admixture and 0.25 wt.% transitional nano-alumina on the fresh properties, the hardened mechanical properties, and self-healing efficiency were examined. The inclusion of mechanically activated fly ash caused a slight delay in the setting time compared with the reference mortar. However, incorporating 1 wt.% crystalline admixture into the fly ash-modified mortar resulted in a significant delay in the setting time. The mechanical properties of the modified mortars remained consistent with the expected values for conventional mortars. The highest self-healing efficiency was observed in mortars containing 16 wt.% mechanically activated fly ash and 1 wt.% crystalline admixture, achieving 36 % self-healing efficiency after 28 days, which increased to 89 % after 56 days, and 96% after 90 days of curing. Similarly, mortars incorporating 0.25 wt.% transitional nano-alumina also achieved 96 % self-healing efficiency after 90 days. However, the addition of 0.25 wt.% transitional nano-alumina exhibited a delayed self-healing effect, with only 10 % self-healing efficiency after 28 days and 63 % after 56 days of curing.

**Keywords:** mechanically activated fly ash; mortars; self-healing; circular economy; crystalline admixture; transitional nano-alumina

## ВЛИЈАНИЕ НА МЕХАНИЧКИ АКТИВИРАНА ЛЕТЕЧКА ПЕПЕЛ, КРИСТАЛЕН ДОДАТОК И НАНОАЛУМИНА ВРЗ СВЕЖИТЕ СВОЈСТВА, МЕХАНИЧКИТЕ СВОЈСТВА И САМОЛЕКУВАЊЕТО НА ЦЕМЕНТНИТЕ МАЛТЕРИ

Намалувањето на отпечатокот од јаглероден диоксид (CO<sub>2</sub>) во градежната индустрија е клучна глобална цел во стремежот кон одржливост, особено имајќи предвид дека производството на обичен портланд-цемент (OPC) е значаен фактор за глобалните емисии на CO<sub>2</sub>. Истражени се

бројни напредни технолошки решенија за ублажување на ова влијание, а еден ветувачки пристап е делумната замена на цементот со дополнителни цементни материјали, усогласувајќи се со принципите на циркуларна економија. Целта на оваа студија беше да се развијат зелени малтери со замена на 16 мас.% цемент со механички активирани летечка пепел. Покрај тоа, испитани беа ефектите од додавањето на 1 мас.% кристален додаток и 0,25 мас.% преодна наноалумина врз свежите својства, стврднатите механички својства и ефикасноста на самоллекување. Примената на механички активирани летечка пепел предизвика мало одложување во времето на стврднување во споредба со референтниот малтер. Сепак, примената на 1 мас.% кристален додаток во малтерот модифициран со летечка пепел резултираше со значително одложено време на стврднување. Механичките својства на модифицираните малтери останаа во согласност со очекуваните вредности за конвенционалните малтери. Највисока ефикасност на самоллекување е забележана кај малтерите кои содржат 16 мас.% механички активирани летечка пепел и 1 мас.% кристален додаток, постигнувајќи 36 % ефикасност на самоллекување по 28 дена, која се зголеми на 89 % по 56 дена и на 96 % по 90 дена третман. Слично, малтерите што содржат 0,25 мас.% преодна наноалумина исто така постигнаа 96 % ефикасност на самоллекување по 90 дена. Сепак, додавањето на 0,25 мас.% преодна наноалумина покажа одложен ефект на самоллекување, со само 10% ефикасност на самоллекување по 28 дена и 63 % по 56 дена стврднување.

**Клучни зборови:** механички активирани летечка пепел; малтери; самоллекување; кружна економија; кристален додаток; преодна наноалумина

## 1. INTRODUCTION

The construction industry accounts for approximately 11 % of global greenhouse gas (GHG) emissions, with cement production, particularly the clinker manufacturing process, representing this sector's primary contributor to carbon emissions. In recent years, there has been an intensification of efforts to reduce carbon dioxide (CO<sub>2</sub>) emissions from cement and concrete production. One of the most effective and widely accepted approaches is partially replacing cement with supplementary cementitious materials (SCMs). This strategy helps lower the clinker content in cement-based materials, thereby reducing overall GHG emissions. Among the various SCMs, fly ash, a by-product of coal combustion in thermal power plants, is one of the most commonly used alternatives due to its pozzolanic activity and sustainability benefits.<sup>1-4</sup>

The incorporation of fly ash in cement-based materials provides dual benefits: it reduces the amount of fly ash requiring disposal as industrial waste, and it enhances the material's performance due to its pozzolanic properties. The influence of fly ash on mortar strength is primarily determined by its physical characteristics, including particle size distribution and specific surface area, as well as its chemical and mineralogical composition. While raw fly ash can be used directly in cement-based materials, its hydraulic properties and pozzolanic reactivity can be significantly improved through mechanical activation, transforming it into a higher-value, more reactive material.<sup>5</sup>

Mechanical activation is the most effective method for enhancing fly ash properties, as it re-

duces the particle size, significantly increases its specific surface area, and decreases its crystallinity.<sup>6</sup> Numerous studies have investigated the mechanical activation of fly ash, particularly its use in hydraulic binders (such as Portland cement) or geopolymers.<sup>5,7</sup> Based on prior research, mechanically activated fly ash can be incorporated into cement at higher proportions without negatively affecting mechanical properties. This ability is due to the increased reactivity that results from the particle size reduction and an increased surface area, which enhance the pozzolanic reactivity of fly ash. The altered particle morphology and size distribution accelerate dissolution-precipitation reactions, leading to the development of a denser microstructure with improved mechanical properties of the final product.<sup>8</sup> Additionally, fly ash contributes to the longevity of the product due to its ability to act as a mineral addition for autogenous self-healing, which extends the service life of cement-based materials.<sup>9</sup>

The construction industry is moving forward to a more innovative and sustainable route. Self-healing can play a vital role in the reduction of industry-related environmental impact by providing construction materials with a prolonged service life.<sup>10</sup> The concept of self-healing is widely applied to various materials in civil engineering, such as concrete, the most widely used manmade material,<sup>10</sup> mortars,<sup>11</sup> and geopolymers, an alternative cementing material with a lower carbon footprint,<sup>12</sup> among others. Despite advancements in material design, crack formation remains unavoidable, potentially compromising the structural integrity of the entire system.<sup>13</sup> Cracks can form at any stage

during the service life of cement-based materials,<sup>14</sup> creating pathways for moisture, salts, chlorides, and other aggressive agents to infiltrate and degrade the internal structure.<sup>15</sup> Various factors contribute to crack formation, including climate change effects (temperature fluctuations and extreme weather), geological factors (seismic activity and soil settlement), drying shrinkage, freeze-thaw cycles, and thermal stress-induced volume changes, among others.<sup>16</sup> A promising solution to mitigate microcracks and to prevent their propagation is the integration of self-healing mechanisms within cement-based materials. These mechanisms enhance material longevity, reduce maintenance costs, and contribute to more sustainable and resilient infrastructure. The selection of an appropriate self-healing mechanism depends on several key factors, including material composition, structural age, exposure conditions, and the properties of the self-healing agent, which can be intrinsic (autogenous) or extrinsic (autonomous).<sup>13</sup> The concept of self-healing is defined in multiple ways: (i) the ability of the material to initiate the hydration processes, leading to crack sealing;<sup>17</sup> (ii) the capacity of the material to repair cracks autonomously, without human intervention;<sup>18</sup> and (iii) the capability of the material to partially or fully restore its mechanical properties after damage.<sup>19</sup> Various effective strategies are employed to enable these self-healing processes, including the dispersion of polymers, the incorporation of fibers, bacterial-based healing agents, crystalline admixtures, mineral additives, and nanomaterials.<sup>13,20</sup>

Crystalline admixtures (CAs) are a specialized class of additives comprising a proprietary blend of active chemicals that significantly reduce water permeability and enhance the self-healing capacity of cement-based materials. These commercial products have confidential formulations, and they typically do not exceed 1 wt.% of the cement weight. In the presence of water, CAs trigger chemical reactions that lead to the formation of water-insoluble precipitates within pores and cracks. Depending on the crystalline promoter, these precipitates are primarily composed of modified calcium silicate hydrate (C-S-H) or calcium carbonate (CaCO<sub>3</sub>), contributing to microstructural densification and significantly improving water resistance.<sup>9,21</sup>

In recent years, significant research efforts have been dedicated to the integration of nanomaterials in the construction industry. Additionally, they can be regarded as a sustainable option, given that the manufacturing processes of nanomaterials contribute minimally to carbon emis-

sions.<sup>22</sup> Various types of nanomaterials, including nano-silicon dioxide (SiO<sub>2</sub>), nano-titanium dioxide (TiO<sub>2</sub>), nano-clay, nano-aluminum oxide (Al<sub>2</sub>O<sub>3</sub>), carbon nanotubes (CNTs), and graphene oxide, have been studied extensively for their ability to enhance the properties of cement-based materials. The application of nanomaterials to enhance self-healing efficiency is a relatively novel concept, with ongoing research aimed at elucidating their role as healing agents. Due to their ultrafine particle size and high specific surface area, nanomaterials, when incorporated into cement-based composites, create additional nucleation sites for the formation of C-S-H gel, the primary binding phase in cement hydration. This nucleation effect accelerates hydration reactions, leading to a denser microstructure with improved mechanical properties and reduced permeability.<sup>23</sup>

Nano-alumina has been used in different cement-based products in construction. Farzadnia *et al.*<sup>24</sup> showed that the addition of 1 % nano-alumina with the average size of 13 nm enhances the compressive strength of high strength mortars by up to 16 % at room temperature and the residual strength by up to 800°C. Higher amounts of nano-alumina (more than 2 %) lower the compressive strength of mortars back to its original strength due to agglomeration and water absorption issues. Cuenca *et al.*<sup>25</sup> examined the impact of alumina nano-fibers (0.25 wt.% by cement mass) on the mechanical performance and durability of ultra-high performance fiber-reinforced cementitious concrete, particularly in extreme conditions. The findings highlight their effectiveness in enhancing crack sealing and self-healing capacity by improving flexural and tensile mechanical behavior. Alumina nano-fibers improve durability by controlling cracking at an early stage and promoting hydration reactions due to their hydrophilic nature, ultimately enhancing mechanical recovery and water permeability resistance. Shao *et al.*<sup>26</sup> showed that the addition of 5 % nano  $\gamma$ -alumina to Portland cement enhances long-term strength by promoting the formation of AFm phases (monosulfate and monocarbonate), which increase solid volume and refine pore structure. This process reduces porosity, the sulfur species concentration, and the portlandite content while slightly increasing bound water. However, nano-alumina dissolves slowly, contributing to a gradual strength improvement over time.

Based on a review of the literature, there has been relatively little research on the use of transitional nano-alumina in construction materials, especially for mortars and concrete, compared with other types of nanoparticles. Zhou *et al.*<sup>27</sup> studied

the impact of transitional aluminas on hydration kinetics, phase assemblage of Portland cement, and the alkali-silica reaction (ASR) prevention. Transitional aluminas, derived from annealed reactive alumina exhibit reduced reactivity as the annealing temperature increases. As the temperature increases, reactive alumina gradually transforms from  $\gamma$ -alumina to  $\delta$ - and  $\theta$ -alumina before the final conversion of  $\alpha$ -alumina as the most thermodynamically stable phase.  $\gamma$ -alumina is a metastable phase (polymorph) and is considered to be highly reactive. Highly reactive transitional aluminas promote katoite formation, increasing the Al concentration in the pore and enhancing prevention of the ASR. Their rapid dissolution significantly affects early cement hydration. In contrast, transitional aluminas with low reactivity act as fillers, accelerating cement hydration without major chemical interactions.

This study explored the use of fly ash as an SCM to promote a sustainable approach to utilizing locally available resources<sup>28</sup> in the design of green mortars. The focus was on mortars in which 16 wt.% of cement was replaced with mechanically activated fly ash. The synergistic effects of crystalline admixtures and transitional nano-alumina (0.25 wt.%) on modified fly ash mortars were ana-

lyzed in terms of the fresh properties, mechanical performance, and self-healing capabilities. This research addresses a key literature gap regarding the use of transitional nano-alumina in green mortar design.

## 2. EXPERIMENTAL SECTION

### 2.1. Materials

This study utilized Ordinary Portland Cement (OPC) (CEM I 52.5R) from Cementarnica USJE-TITAN Group (Republic of North Macedonia), fly ash sourced from the REK Bitola thermal power plant, a crystalline admixture (known as Hidrofob Kristal) from the company Ading AD Skopje (Republic of North Macedonia), and transitional nano-alumina supplied by IBU-tec (Germany).

OPC was used as the primary binder in the mortar mixes. Its chemical composition and physical properties are presented in Tables 1 and 2, respectively, while its compressive strength is shown in Table 3. The free calcium oxide (CaO) content was 0.8 wt.%. The OPC data were provided by the manufacturer.

Table 1

*Chemical composition of cement CEM I 52.5R, wt. %*

Cement	SiO <sub>2</sub>	Al <sub>2</sub> O <sub>3</sub>	Fe <sub>2</sub> O <sub>3</sub>	CaO	MgO	K <sub>2</sub> O	Na <sub>2</sub> O
CEM I 52,5R	17.81	5.20	2.76	63.90	2.54	0.81	0.23

Table 2

*Physical characteristics of cement CEM I 52.5R*

Specific surface area (Blaine), cm <sup>2</sup> /g	Sieve residue > 45 $\mu$ m, %	Standard consistency %	Initial setting time min	Final setting time min
4070	2.4	31.2	148	173

Table 3

*Compressive strength of cement CEM I 52.5R*

Age of specimen, days	2	7	28
Compressive strength, MPa	40.6	53.9	63.2

Mechanically activated fly ash was used in the mortar mixes. The raw fly ash was mechanically activated by grinding in a ball mill (Bond Grinding Test Mill, HIRA LABORATORY TESTING EQUIPMENT, Turkey) before utilization. The grinding process was conducted under the follow-

ing conditions: an applied speed of 70 rpm and a milling duration of 40 min, ensuring that the material retained less than 20 % residue on a 32- $\mu$ m sieve.

The chemical composition (in wt.%) of the fly ash after mechanical activation was as follows:

SiO<sub>2</sub>, 51.48; Al<sub>2</sub>O<sub>3</sub>, 21.11; Fe<sub>2</sub>O<sub>3</sub>, 9.30; CaO, 8.06; MgO, 2.81; Na<sub>2</sub>O, 1.26; and loss of ignition (LOI), 0.54. Based on its composition, it is classified as siliceous fly ash.<sup>29</sup> The density of the mechanically activated fly ash was 2.064 g/cm<sup>3</sup>. The mean particle diameter (D<sub>50</sub>) after mechanical activation was 11 μm, and the particle size distribution was unimodal, extending up to 105 μm.

The mineralogical composition of the mechanically activated fly ash consisted of both amorphous and crystalline phases, with quartz, plagioclase, and hematite as the dominant crystalline components.

The morphology of the mechanically activated fly ash particles is shown in Figure 1, highlighting their heterogeneous nature. Typical fly ash cenospheres (1–4 μm)<sup>30</sup> persist even after mechanical activation, which is intended to enhance reactivity.<sup>31</sup> Irregular particles with internal pores (less than 1 μm) and coarse particles exhibiting irregular geometries and sharp edges are also evident.

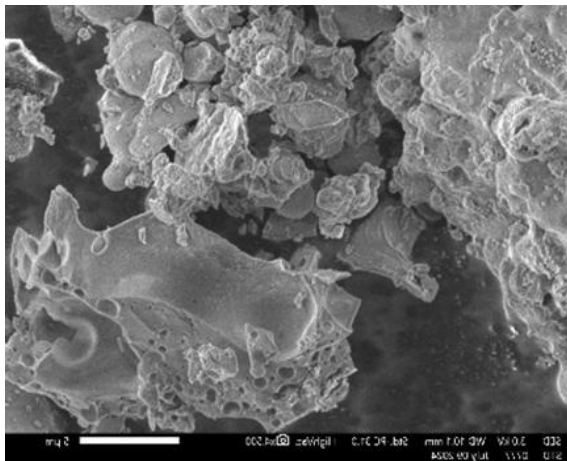


Fig. 1. Morphology of mechanically activated fly ash

Transitional nano-alumina powder (99.98 %) with a specific surface area of 124 m<sup>2</sup>/g was used in this study. The powder was aggregated with dimensions ranging from 100 to 600 nm, while the primary particle size ranged from 5 to 50 nm. The phase composition consisted of the α, δ, γ, and θ phases, commonly referred to as “Greek-letter alumina” or transitional alumina. The δ- and γ-alumina phases were dominant, while θ-alumina (the final metastable transitional phase) and stable α-alumina were present in approximately equal amounts at 10 ± 1 wt.% each.<sup>32</sup>

Four types of mortar were prepared in this study, as shown in Table 4. The first mortar, M1, served as the reference and was formulated as a standard mortar in accordance with EN 196-1.<sup>33</sup> In the other three mortars (M2, M3, and M4), 16 wt.% of OPC was replaced with mechanically activated fly ash. Additionally, M3 contained crystalline admixture (1 wt.% of the total binder content), while M4 included transitional nano-alumina (0.25 wt.% of the total binder content). To minimize the potential agglomeration of nano-alumina particles in fresh samples, the nano-alumina powder was first ultrasonically dispersed in water for 30 min. Then, the resulting dispersion was transferred to a mechanical mixer, where the designed mortar mix was added gradually while stirring. The water-to-cement ratio was maintained at 0.5 for all samples. All mortars were prepared by following the standardized procedure outlined in EN 196-1.<sup>33</sup> The replacement level of mechanically activated fly ash in mortar and the addition of small quantities of transitional nano-alumina were determined based on a comprehensive literature review and prior research findings.

Table 4

Mix design of mortars

Mortar sample	OPC g	CA g	MAFA g	NA g	Standard sand g	Water ml
M1	450	/	/	/	1350	225
M2	378	/	72	/	1350	225
M3	378	4.5	72	/	1350	225
M4	378	/	72	1.125	1350	225

## 2.2. Methods

The chemical composition of fly ash was analyzed using X-ray fluorescence spectroscopy (S8 TIGER WDXRF spectrometer, Bruker, Germany). Its particle size distribution (PSD) was measured

using dry laser granulometry (1090 laser particle size analyzer, Cilas, France). The morphology of fly ash particles was examined via scanning electron microscopy (FEI Quanta 200, JEOL, Japan) with a secondary electron detector and an accelerating voltage of 30 kV under high vacuum.

The fresh properties of the mortar mixes were evaluated according to standard procedures outlined in the EN standards. Specifically, the bulk density of fresh mortar was determined following EN 1015-6.<sup>34</sup> The consistency of the mortar mixtures was assessed by using the flow table method, as specified in EN 1015-3.<sup>35</sup> The air content in fresh mortar was measured according to EN 1015-7.<sup>36</sup> Finally, the initial and final setting times of the mortars were determined using a Vicat apparatus (CONTROLS, Italy) in compliance with EN 480-2.<sup>37</sup>

To evaluate the mechanical properties of mortars, standard prisms (40 × 40 × 160 mm) were prepared in accordance with EN 1015-11.<sup>38</sup> The specimens were cured under moist conditions at 20°C and ≤ 95 % relative humidity for 28 days. The mechanical properties, including compressive and flexural strength, were determined following EN 1015-11.<sup>38</sup>

The flexural strength test was conducted using a three-point bending test, applying the load at a rate of 50 ± 10 N/s until the prism fractured. The compressive strength test was performed on both halves of the fractured prism, with the load applied at a rate of 2400 ± 200 N/s. Both tests were carried out using the E161-01A + E172-01 compression/flexural testing machine (MATEST, Italy). Three specimens from each mortar mix were tested, and the results were averaged.

The self-healing efficiency was assessed by monitoring crack closure through microscopy and measuring capillary water absorption in pre-cracked samples, following the procedure outlined by Stefanovska *et al.*<sup>39</sup> Crack formation was induced using a three-point bending test on mortar specimens aged for 28 days. Then, the cracks were examined and documented using a digital microscope. After crack formation, the specimens were immersed in water to promote autogenous self-healing. This conditioning method was selected based on extensive research that has demonstrated the essential role of excess water in facilitating autogenous self-healing.<sup>40,41</sup> Crack closure was observed and photographed after 7, 14, 21, 28, 56, and 90 days of submersion. The initial crack widths of all specimens ranged from 100 to 600 μm.

To evaluate healing efficiency via capillary water absorption, three types of specimens were tested for each mortar mix: uncracked specimens, specimens with unhealed cracks, and specimens with healed cracks. The conditioning procedures for all specimens were as follows: Uncracked specimens were conditioned by submersion in water for 28 days; unhealed specimens were aged under laboratory conditions for 28 days. Healed specimens were submerged in water and tested after 28, 56,

and 90 days of treatment. Before testing, all specimens were dried in a ventilated oven at 70°C for 7 days. To control water absorption, each specimen was coated with epoxy resin to a height of 20 mm on all sides, leaving only a 2-cm-wide central strip exposed, where the cracks were located. The test was conducted once the resin had fully dried, following the procedure outlined in EN 13057.<sup>42</sup> During testing, specimens were placed on spacers inside a sealed, watertight container and immersed in water to a depth of 2.0 ± 1.0 mm from the base. Before immersion, each specimen was weighed to determine its initial mass. Then, water absorption measurements were taken at 15, 30, 60, 120, 240, and 480 min. The sorption coefficient was determined as the slope of the line in a graph plotting water uptake against the square root of immersion time. The healing efficiency was calculated using the following formula:<sup>43</sup>

$$ISH = \frac{S_{unhealed} - S_{healed}}{S_{unhealed} - S_{uncracked}} * 100$$

where  $S_{unhealed}$  is the sorption coefficient of specimens with an unhealed crack,  $S_{healed}$  is the sorption coefficient of samples with a healed crack, and  $S_{uncracked}$  is the sorption coefficient of samples without a crack.

### 3. RESULTS AND DISCUSSION

#### 3.1. Fresh mortar properties

Figure 2 presents the fresh mortar properties, including bulk density, the air content, consistency, and setting time (initial and final). The bulk density of fresh mortars varied depending on their composition. The modified mortars exhibited a lower density than the reference mortar (M1), which can be attributed to the lower density of mechanically activated fly ash and, most probably, to the crystalline admixture and transitional nano-alumina.

There was no significant difference in the air content among the mortar mixes. Regarding consistency, there was a slight difference between M1 (152 mm) and M2 (150 mm), while M3 exhibited an increased consistency of up to 160 mm, likely due to the plasticizing effect of the crystalline admixture. In contrast, M4 showed a reduced consistency (145 mm), attributed to the presence of transitional nano-alumina, which affects workability as expected by nano materials addition.<sup>44</sup>

The setting time was also influenced by the mortar composition. The addition of mechanically

activated fly ash in M2 caused a slight delay in both the initial and final setting times compared M1, due to the slower hydration reaction of fly ash compared with OPC.<sup>45</sup> M3 presented a more pronounced delay in the setting time, a phenomenon attributed to the retarding properties of the crystalline admixture. M4 also exhibited a slight delay in the setting time, suggesting that transitional nano-alumina also exerts a retarding effect on the setting

time, although less pronounced than the crystalline admixture. The influence of transitional nano-alumina on fresh mortar properties can be explained by its high surface area-to-volume ratio, high chemical reactivity, and pozzolanic properties, which modify the hydration kinetics and rheological behavior of the mix.<sup>46</sup> The initial and final setting times increased, indicating a delayed hydration process.

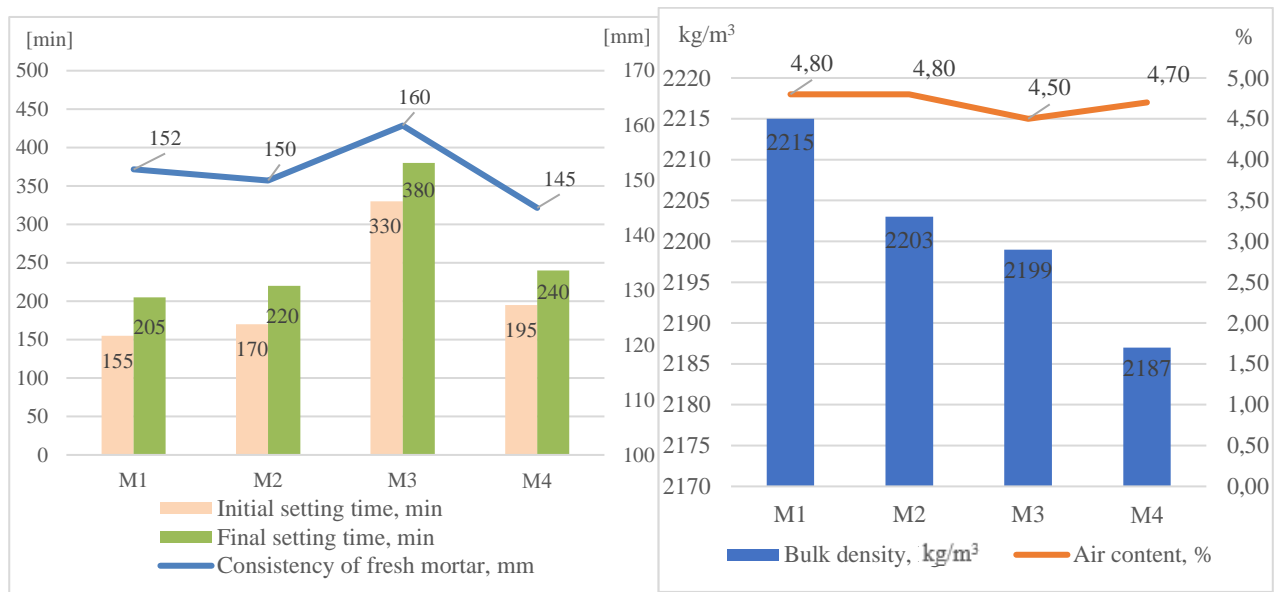


**Fig. 2.** Graphical presentation of fresh mortar properties: setting time and consistency of fresh mortar (left); bulk density and air content (right)

### 3.2. Mechanical properties of the mortars

Figure 3 illustrates the mechanical properties of mortars, specifically flexural strength and compressive strength, after 2 and 28 days of curing. The modified mortars (M2, M3, and M4) exhibited lower mechanical properties after 2 days of curing, which can be attributed to the reduced cement content and the slower hydration rate of mechanically activated fly ash compared with OPC. However, after 28 days of curing, the mechanical properties of all modified mortars significantly increased, reaching values comparable to those of M1 (the reference mortar).

Compared with a previous study that used as-received fly ash in the mix design,<sup>39</sup> the present study demonstrated that mechanically activated fly ash has a more beneficial effect on the mechanical properties of mortar. Specifically, the use of mechanically activated fly ash increased compressive strength by 4 %, whereas the mortar containing as-received fly ash exhibited an 11 % decrease in compressive strength. This enhancement is attributed to the increased specific surface area of fly ash particles after mechanical activation. The activation process produces fly ash

particles with a larger surface area and finer particle size, making them more comparable to cement particles. As a result, the reactivity of fly ash is enhanced, improving its pozzolanic effect, as the silica content in fly ash particles becomes more readily available for reaction.<sup>47</sup> In the cement matrix, fly ash reacts with available lime and alkali, forming additional cementitious compounds. The fundamental pozzolanic reaction is:



This reaction leads to C-S-H forming, which serves as an additional binder, allowing the cementitious material to gain strength over time, even after OPC has reached its final strength. Cement materials containing fly ash typically continue developing their final strength over 90 days of curing.<sup>48</sup> This phenomenon is further supported by Ulaz *et al.*,<sup>49</sup> who reported that the mechanical properties improve over time due to the continuous development of hydration products. Additionally, prolonged pozzolanic reactions contribute to a denser microstructure, forming hydrated gels of C-

S-H (calcium silicate hydrate) and calcium aluminate hydrate (C-A-H) types. These gels are generated by the dissolution of pozzolanic phases such as  $\text{SiO}_2$  and  $\text{Al}_2\text{O}_3$  from fly ash and transitional nano-alumina, which react with calcium ions

( $\text{Ca}^{2+}$ ) from calcium hydroxide ( $\text{Ca}(\text{OH})_2$ ) in the presence of water.<sup>49</sup> On the other hand, the presence of  $\gamma$ -nano-alumina enhances long-term strength, as reported by Shao *et al.*<sup>26</sup>

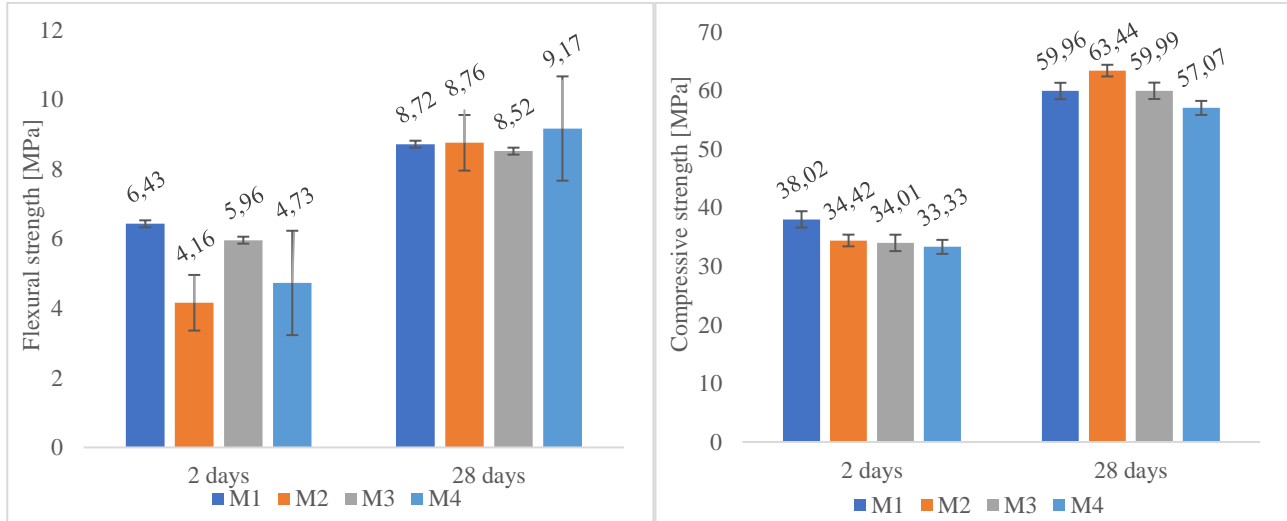


**Fig. 3.** Graphical representation of mechanical properties over time for cement mortars: flexural strength (left) and compressive strength (right)

### 3.3. Microscopic investigation of crack reduction

Figure 4 presents image of cracks and the reduction in crack width for a representative section of each mortar mix over 90 days of treatment. The initial crack width for all representative cracks is approximately  $400 \pm 20 \mu\text{m}$ . However, it is im-

portant to note that crack width varies along the length of each specimen, with initial values ranging from 100 to 600  $\mu\text{m}$ . Additionally, Fig. 5 illustrates the progressive closure of the crack along its entire length during the self-healing process in M4 with crack width reduction measured at 7, 14, 21, 28, 56, and 90 days.

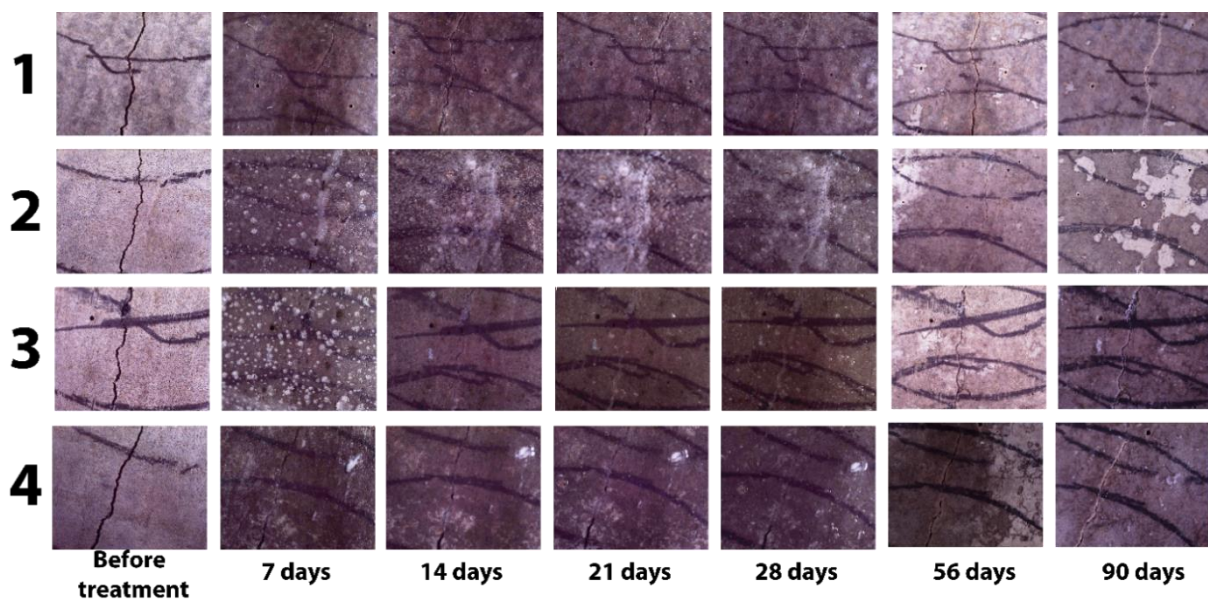


**Fig. 4.** Crack width reduction for a representative section of each mortar

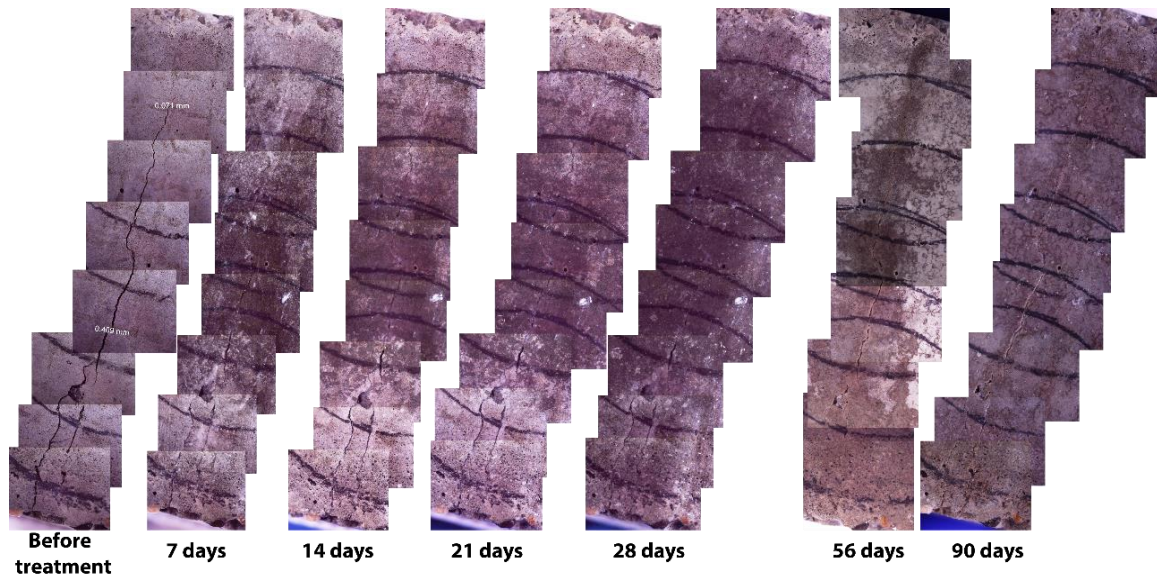


Fig. 5. Crack width reduction along the entire crack length of M4

In all cases, there was a notable crack width reduction, particularly after 90 days of treatment. For M2 and M4, partial crack closure was evident after 90 days of treatment, indicating an active self-healing process. However, for M3, cracks reopened after 28 days of treatment due to the fragility of the specimen. This issue could potentially be mitigated by reinforcing the specimens with fibers, which would enhance structural integrity and minimize crack propagation. Although the crack reopened in M3, the self-healing process remained active, leading to a further crack reduction between 56 and 90 days of treatment. This suggests that even in cases of structural weakness, continued exposure to favorable healing conditions (such as water immersion) facilitates ongoing autogenous self-healing.

### 3.4. Self-healing efficiency

Figures 6–9 illustrate the self-healing efficiency of each mortar mix, determined through capillary water absorption testing. The healing efficiency was calculated by using the slopes of the water absorption curves.<sup>34</sup> After 28 days of water conditioning, M1 exhibited a healing efficiency of 10 %. In comparison, M2 and M3 achieved an efficiency of 33 % and 36 %, respectively, indicating improved self-healing properties. However, M4, which contained transitional nano-alumina, showed no significant self-healing effect, maintaining a healing efficiency of 10 %, similarly to M1. Based on these findings, M3 demonstrated the highest self-healing efficiency after 28 days, likely

due to the synergistic effect of crystalline admixture and mechanically activated fly ash. The self-healing efficiency observed for M1 is attributed to the natural autogenous healing mechanism inherent in cementitious materials. This process enables the material to repair itself independently by detecting cracks, triggering the healing process, facilitating crack closure, and ultimately sealing the damaged areas.<sup>11</sup> With continued treatment, the self-healing efficiency increased as follows: for M1, it reached 56 % after 56 days and 83 % after 90 days; for M2, it reached 87 % after 56 days and 90 % after 90 days; for M3, it increased to 89 % after 56 days and 96 % after 90 days; and for M4, it reached 63 % after 56 days and 96 % after 90 days.

Cement-based materials with mineral additions, such as fly ash in M2, can heal cracks through stimulated autogenous self-healing. This process relies on the continuous hydration of unreacted cement particles and the precipitation of  $\text{CaCO}_3$ . These mechanisms occur simultaneously until all anhydrate cement particles are depleted. Additionally, the dissolution and subsequent carbonation of  $\text{Ca}(\text{OH})_2$  can persist over an extended period, as long as  $\text{Ca}^{2+}$  is present in the system. The presence of water is a crucial factor, as it initiates and sustains the self-healing process.<sup>40,50,51</sup> Among all tested mortars, M3 exhibited the highest self-healing efficiency over 90 days. Crystalline admixture acts as an additional stimulator for autogenous self-healing, enhancing the reaction kinetics.<sup>25</sup> When combined with mechanically activated fly ash, crystalline admixture accelerates the hydration process, leading to a faster and more efficient self-

healing response. Furthermore, in the presence of water, crystalline admixtures form precipitates that fill micropores and cracks, increasing the material's density and significantly reducing its water permeability.<sup>21</sup>

Cuenca *et al.*<sup>52</sup> described the role of crystalline admixture in concrete as a stimulant for both self-healing and self-sealing processes. When exposed to high humidity, crystalline admixture undergoes chemical reactions that lead to the formation of insoluble, needle-like crystals within hairline cracks, pores, and capillaries. This phenomenon is attributed to the hydrophilic nature of crystalline admixtures, which facilitate moisture absorption and enhance the material's ability to self-seal. Moreover, the morphology and reduced particle size of mechanically activated fly ash accelerate dissolution-precipitation reactions, increasing its reactivity. As a result, this enhanced reactivity promotes a more efficient and active self-healing process in mortar.<sup>53</sup>

Transitional nano-alumina exhibited a delaying effect on the self-healing capacity of mortars. During the first 28 days, its impact on self-healing was minimal (10 %) and comparable to the natural autogenous healing observed in M1 (the reference mortar). Specifically, transitional nano-alumina demonstrated a retarding effect compared with crystalline admixture, achieving only 63 % self-healing efficiency after 56 days, whereas M3 reached a self-healing efficiency of 89 % under the same conditions. However, after 90 days, the self-healing efficiency of M4 increased significantly, ultimately reaching 96 %, the same level as M3. The addition of nano-alumina in cement-based products promotes the formation of C-(A)-S-H gels, which influence the setting time and facilitate the efficient injection of silica or binding agents into the hydration gel's microstructure for refinement.<sup>54</sup> This delayed yet substantial improvement is likely due to the presence of metastable phases within the transitional nano-alumina, which gradually contribute to the self-healing process over time.

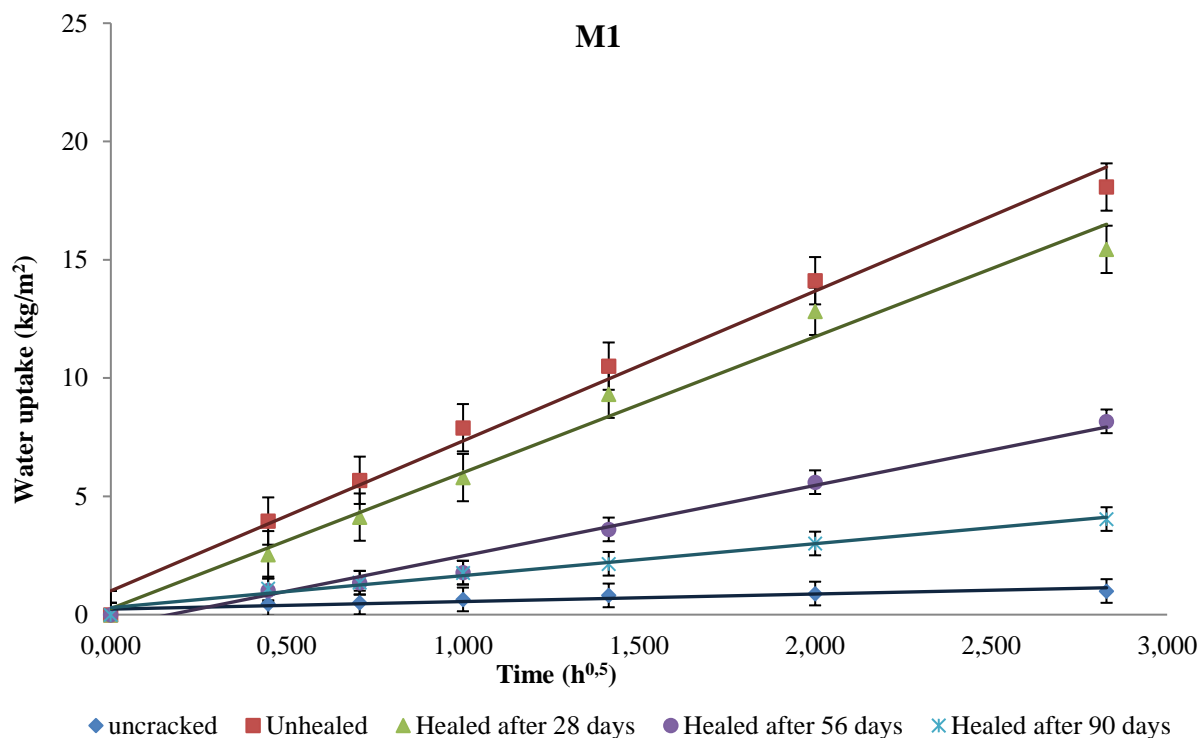


Fig. 6. Water uptake in relation to the square root of the time for M1

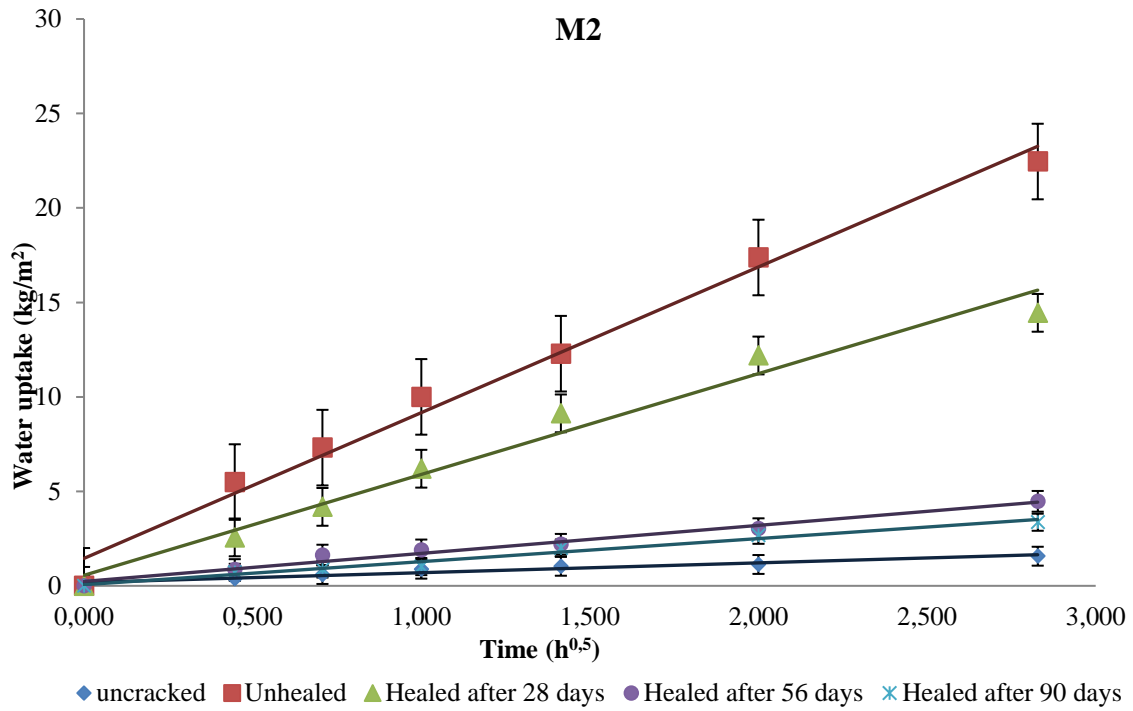


Fig. 7. Water uptake in relation to the square root of the time for M2

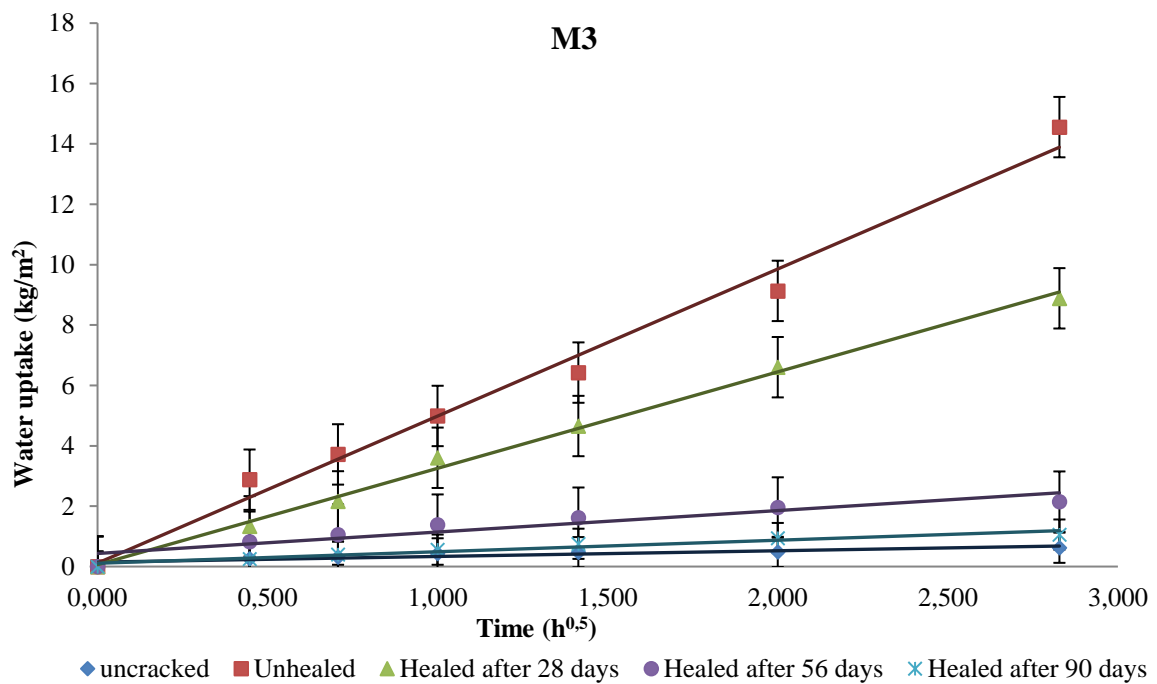


Fig. 8. Water uptake in relation to the square root of the time for M3

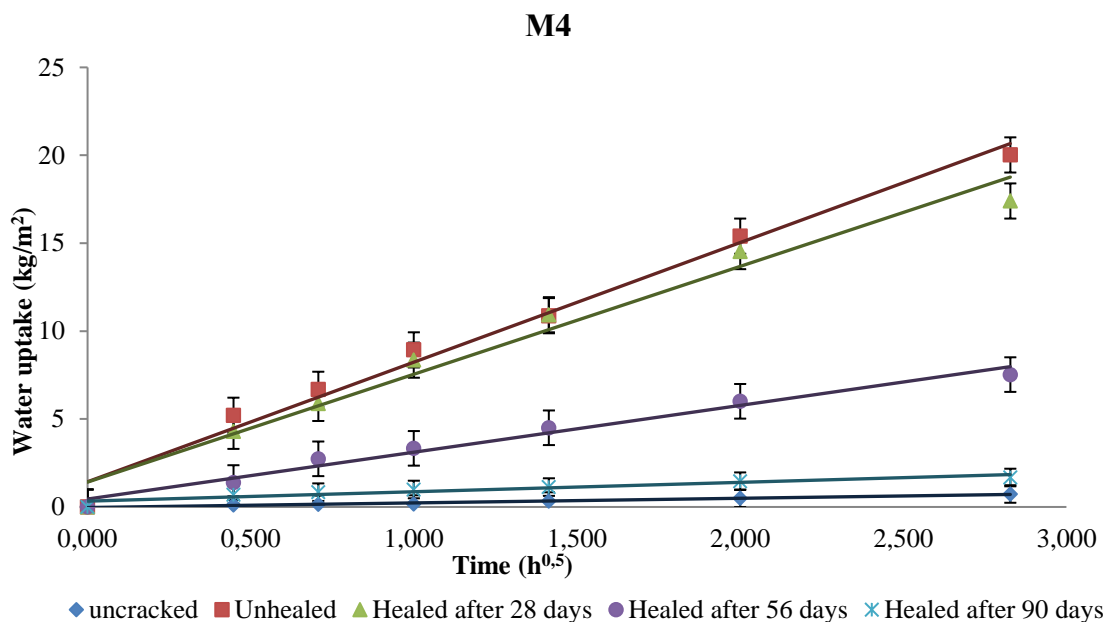


Fig. 9. Water uptake in relation to the square root of the time for M4

#### 4. CONCLUSION

This study provides valuable insights into sustainable construction practices, with the following key conclusions:

Replacing 16 wt.% of cement with mechanically activated fly ash in all modified mortars, along with addition of 1 wt.% crystalline admixture (in mortar M3) and 0.25 wt.% transitional nano-alumina (in mortar M4), significantly affected the fresh properties of the mortars. Specifically, the synergistic effect of mechanically activated fly ash and crystalline admixture most notably influences the fresh properties, particularly by enhancing consistency and drastically delaying the setting time. This combination results in a more workable mortar mix and provides greater flexibility during application.

The flexural and compressive strength of the modified mortars did not change significantly. All mortars meet the expected performance standards for conventional mortars.

Regarding self-healing, mechanically activated fly ash (16 wt.% as a substitution for OPC) in M2 positively influenced the process, while the combination of mechanically activated fly ash and 1 wt.% crystalline admixture (M3) resulted in the best self-healing outcomes at 28, 56, and 90 days. The addition of 0.25 wt.% transitional nano-alumina (M4) showed a delayed effect on self-healing but ultimately achieved a self-healing efficiency of 96 % after 90 days, the same as M3. These findings underscore the effectiveness of mechanically activated fly ash, crystalline admixture, and transitional nano-alumina in enhancing the

self-healing process in mortars, particularly with extended treatment periods.

Substituting 16 wt.% of cement with mechanically activated fly ash aligns with key principles of green construction, including circularity, reduced raw material consumption, and cost savings. Moreover, this substitution provides dual environmental benefits: it promotes the concept of a circular economy by utilizing industrial by-products as secondary raw materials, and it helps to reduce CO<sub>2</sub> emissions by lowering the cement content in the mortar.

The observed improvements in crack width reduction and self-healing efficiency hold significant implications for real-world applications in sustainable construction. Namely, the positive effects can be mainly seen in the durability enhancement in infrastructure, reduced maintenance and lifecycle costs, and low carbon construction. The ability of modified mortars, particularly M3 and M4, to achieve up to 96% self-healing efficiency after 90 days demonstrates their potential to enhance the longevity and resilience of mortars. By reducing crack width over time, these materials can effectively prolong service life and reduce maintenance costs.

Future studies should focus on comprehensive durability assessments and life cycle analysis to optimize their possibility for practical implementation in the civil engineering and construction industries.

**Acknowledgment.** This study received funding from the Ministry of the Economy of the Republic of North Macedonia, contract No. 18-4427/3 from 21.12.2023.

## REFERENCES

- (1) World Green Building Council  
<https://worldgbc.org/advancing-net-zero/embodied-carbon/> (accessed 2024 -09 -14).
- (2) Xu, G.; Shi, X., Characteristics and Applications of Fly Ash as a Sustainable Construction Material: A state-of-the-art review. *Resour. Conserv. Recycl.* **2018**, *136*, 95–109. <https://doi.org/10.1016/j.resconrec.2018.04.010>
- (3) Hemalatha, T.; Ramaswamy, A., A Review on Fly Ash Characteristics – Towards Promoting High Volume Utilization in Developing Sustainable Concrete. *J. Clean. Prod.* **2017**, *147*, 546–559. <https://doi.org/10.1016/j.jclepro.2017.01.114>
- (4) CE Center Circular Economy Policy Research Center, **2019**, *CO<sub>2</sub> Mineralization for Sustainable Construction*, [https://circulareconomy.europa.eu/platform/sites/default/files/5-co2-mineralisation-for-sustainable-construction-materials-nl\\_1.pdf](https://circulareconomy.europa.eu/platform/sites/default/files/5-co2-mineralisation-for-sustainable-construction-materials-nl_1.pdf) (accessed 2024 -09 -14).
- (5) Klima, K. M.; Schollbach, K.; Brouwers, H. J. H.; Yu, Q., Thermal and Fire Resistance of Class F Fly Ash Based Geopolymers. A review., *Constr. Build. Mater.* **2022**, *323*, 126529. <https://doi.org/10.1016/j.conbuildmat.2022.126529>
- (6) Akmalaiuly, K.; Berdikul, N.; Pundienė, I.; Pranckevičienė, J., The Effect of Mechanical Activation of Fly Ash on Cement-Based Materials Hydration and Hardened State Properties, *Materials* **2023**, *16* (8), 2959. <https://doi.org/10.3390/ma16082959>
- (7) Ez-zaki, H.; Diouri, A.; Maher, M.; Aidi, A.; Guedira, T., Effect of Mechanical Activation of Fly Ash Added to Moroccan Portland Cement, *MATEC Web Conf.* **2018**, *149*, 01074. <https://doi.org/10.1051/mateconf/201814901074>
- (8) Sun, Y.; Wang, Z. H.; Park, D. J.; Kim, W. S.; Kim, H. S.; Yan, S. R.; Lee, H. S., Analysis of the Isothermal Hydration Heat of Cement Paste Containing Mechanically Activated Fly Ash, *Thermochim. Acta* **2022**, *715*, 179273. <https://doi.org/10.1016/j.tca.2022.179273>
- (9) De Belie, N.; Gruyaert, E.; Al-Tabbaa, A.; Antonaci, P.; Baera, C.; Bajare, D.; Darquennes, A.; Davies, R.; Ferrara, L.; Jefferson, T.; Litina, C.; Miljevic, B.; Otlewska, A.; Ranogajec, J.; Roig-Flores, M.; Paine, K.; Lukowski, P.; Serna, P.; Tulliani, J.-M.; Jonkers, H., A Review of Self-Healing Concrete for Damage Management of Structures, *Adv. Mat. Interfaces* **2018** *5* (17), 1800074. <https://doi.org/10.1002/admi.201800074>
- (10) Mohamed, A.; Zhou, Y.; Bertolesi, E.; Mengmei Liu, M.; Liao, F.; Fan, M., Factors Influencing Self-Healing Mechanisms of Cementitious Materials: A review, *Constr. and Build. Mater.* **2023**, *393*, 131550. <https://doi.org/10.1016/j.conbuildmat.2023.131550>
- (11) Lefever, G.; Charkieh, A. S.; Abbass, M.; Van Hemelrijck, D.; Snoeck, D.; Aggelis, D. G., Ultrasonic Evaluation of Self-Healing Cementitious Materials with Superabsorbent Polymers: Mortar vs. Concrete, *Dev. Built Environ.* **2023**, *13*, 100112. <https://doi.org/10.1016/j.dibe.2022.100112>
- (12) Zheng, D.; Ulerio II, G.; Denduluri, V. S.; Juenger, M.; Van Oort, E., Permeability and Self-Healing Behavior of Alkali Activated Geopolymers for Well Cementing Applications, *Geoenergy Sci. Eng.* **2024**, *243*, 213265. <https://doi.org/10.1016/j.geoen.2024.213265>
- (13) Deeba, S.; Ammasi, A. K., State-of-the-Art Review on Self-Healing in Mortar, Concrete, and Composites. *Case Stud. Constr. Mater.* **2024**, *20*, e03298. <https://doi.org/10.1016/j.cscm.2024.e03298>
- (14) Wang, J. Y.; De Belie, N.; Verstraete, W., Diatomaceous Earth as a Protective Vehicle for Bacteria Applied for Self-Healing Concrete, *J. Ind. Microbiol. Biotech.* **2012**, *39*, 567–577. <https://doi.org/10.1007/s10295-011-1037-1>
- (15) Ismail, M.; Toumi, A.; François, R.; Gagn'è, R., Effect of Crack Opening on the Local Diffusion of Chloride in Inert Materials, *Cem. Concr. Res.* **2004**, *34*, 711–716. <https://doi.org/10.1016/j.cemconres.2003.10.025>
- (16) Kan, L. L.; Shi, H. S.; Sakulich, A. R.; Li, V. C., Self-Healing Characterization of Engineered Cementitious Composite Materials, *ACI Mater. J.* **2010**, *107*, 617–624. <https://doi.org/10.14359/51664049>
- (17) Jakhrani, S. H.; Qudoos, A.; Gi Kim, H.; Kyu Jeon, I.; Suk Ryou, J., Review on the Self-Healing Concrete-Approach and Evaluation Techniques, *J. Ceram. Process. Res.* **2019**, *20*, 1–18. <https://doi.org/10.36410/jcpr.2019.20.1>
- (18) Li, V. C.; Herbert, E., Robust Self-Healing Concrete for Sustainable Infrastructure, *J. Adv. Concr. Technol.* **2012**, *10*, 207–218. <https://doi.org/10.3151/jact.10.207>
- (19) Mahmoodi, S.; Sadeghian, P., Self-healing concrete: A Review of Recent Research Developments and Existing Research Gaps, *Annu. Conf. – Can. Soc. Civ. Eng.* **2019**, 1–10.
- (20) Lefever, G.; Aggelis D. G.; De Belie, N.; Van Hemelrijck, D.; Snoeck, D., 4 – Nanomaterials in Self-Healing Cementitious Composites, *Nano-Tailored Multi-Functional Cementitious Composites.* **2022**, 141–159. <https://doi.org/10.1016/B978-0-323-85229-6.00013-5>
- (21) *Report on Chemical Admixtures for Concrete*, ACI Committee 212, American Concrete Institute (ACI), 2010, Ch. 15.
- (22) Liu, C.; He, X.; Deng, X.; Wu, Y.; Zheng, Z.; Liu, J.; Hui, D., Application of Nanomaterials in Ultra-High Performance Concrete: A review. *Nanotechnol. Rev.* **2020**, *9* (1), 1427–1444. <https://doi.org/10.1515/ntrev-2020-0107>
- (23) Goyal, R.; Verma, V. K.; Singh, N., Nanomaterials Based Self-Healing Concrete, *Mater. Today: Proc.* **2023**. <https://doi.org/10.1016/j.matpr.2023.03.553>
- (24) Farzadnia, N.; Abang Ali, A. A.; Demirboga, R., Characterization of High Strength Mortars with Nano Alumina at Elevated Temperatures. *Cem. Concr. Res.* **2013**, *54*, 43–54. <https://doi.org/10.1016/j.cemconres.2013.08.003>
- (25) Cuenca, E.; D'Ambrosio, L.; Lizunov, D.; Tretjakov, A.; Volobujeva, O.; Ferrara, L., Mechanical Properties and Self-Healing Capacity of Ultra High Performance Fibre Reinforced Concrete with Alumina Nano-Fibres: Tailoring Ultra High Durability Concrete for Aggressive Exposure Scenarios, *Cem. Concr. Compos.* **2021**, *118*, 103956. <https://doi.org/10.1016/j.cemconcomp.2021.103956>
- (26) Shao, Q.; Zheng, K.; Zhou, X.; Zhou, J.; Zeng, X., Enhancement of Nano-Alumina on Long-Term Strength of Portland Cement and the Relation to Its Influences on

- Compositional and Microstructural Aspects. *Cem. Concr. Comp.* **2019**, *98*, 39–48. <https://doi.org/10.1016/j.cemconcomp.2019.01.016>
- (27) Zhou, J.; Chen, L.; Liu, Z.; He, F.; Zheng, K., Effect of Transitional Aluminas on Portland Cement Hydration, Phase Assemblage and the Correlation to ASR Preventing Effectiveness. *Cem. Concr. Res.* **2021**, *151*, 106622. <https://doi.org/10.1016/j.cemconres.2021.106622>
- (28) Scrivener, K. L.; Nonat, A., Hydration of Cementitious Materials, Present and Future. *Cem. Concr. Res.* **2011**, *41* (7), 651–665. <https://doi.org/10.1016/j.cemconres.2011.03.026>
- (29) Fidanchevski, E.; Angjusheva, B.; Jovanov, V.; Murtanovski, P.; Vladiceska, Lj.; Aluloska, N. S.; Nikolic, J. K.; Ipavec, A.; Šter, K.; Mrak, M.; Dolenc, S., Technical and Radiological Characterization of Fly Ash and Bottom Ash from Thermal Power Plant, *J. Radioanal. Nucl. Chem.* **2021**, *330*, 685–694. <https://doi.org/10.1007/s10967-021-07980-w>
- (30) Strzałkowska, E., Morphology and Chemical Composition of Mineral Matter Present in Fly Ashes of Bituminous Coal and Lignite, *Int. J. Environ. Sci. Technol.* **2021**, *18*, 2533–2544. <https://doi.org/10.1007/s13762-020-03016-0>
- (31) Pavlík, Z.; Záleská, M.; Pavlíková, M.; Pivák, A.; Nábělková, J.; Lauermannová, A.-M.; Jankovský, O.; Jiříčková, A.; Pilař, L.; Sedmidubský, D., Eco-Friendly Construction Mortars for Heavy Metals Immobilization – Effect of Partial PC Replacement by Lignite-Based Fly Ash and Prolonged High Humidity Curing on Physical and Chemical Parameters, *J. Build. Eng.* **2024**, *97*, 110919. <https://doi.org/10.1016/j.job.2024.110919>
- (32) Bossert, J.; E. Fidancevska, E., Effect of Mechanical Activation on the Sintering of Transition Nanoscaled Alumina, *Sci. Sinter.* **2007**, *39*, 117–125. <https://doi.org/10.2298/SOS0702117B>
- (33) BS EN 196-1: (*Method of Testing Cement*) Determination of strength.
- (34) EN 1015-6: (*Methods of test for mortar for masonry*). Determination of bulk density of fresh mortar.
- (35) EN 1015-3: (*Methods of test for mortar for masonry*). Determination of consistence of fresh mortar.
- (36) EN 1015-7: (*Methods of test for mortar for masonry*). Determination of air content of fresh mortar.
- (37) EN 480-2: (*Admixtures for concrete, mortar and grout - Test methods*). Determination of setting time.
- (38) EN 1015-11: (*Methods of test for mortar for masonry*). Determination of flexural and compressive strength of hardened mortar.
- (39) Stefanovska, I.; Fidanchevski, E., Self-Healing of Cement Mortars Based on Fly Ash and Crystalline Admixture, *MATEC Web Conf.* **2023**, *378*, 02018. <https://doi.org/10.1051/mateconf/202337802018>
- (40) Van Tittelboom, K.; De Belie, N., Self-Healing in Cementitious Materials — A review, *Materials* **2013**, *6*, 2182–2217. <https://doi.org/10.3390/ma6062182>
- (41) Termkhajornkit, P.; Nawa, T.; Yamashiro, Y.; T., Saito, T., Self-Healing Ability of Fly Ash–Cement Systems, *Cem. Concr. Compos.* **2009**, *31*, 195–203. <https://doi.org/10.1016/j.cemconcomp.2008.12.009>
- (42) EN 13057: (*Products and systems for the protection and repair of concrete structures – Test methods*). Determination of resistance of capillary absorption
- (43) Ferrara, L.; Asensi, E. C.; Lo Monte, F.; Flores, M. R.; Moreno, M. S.; Snoeck, D.; Van Mullem, T.; De Belie, N., Experimental Characterization of the Self-Healing Capacity of Cement Based Materials: An overview, *Proceedings.* **2018**, *2*, 454. <https://doi.org/10.3390/ICEM18-05322>
- (44) Quercia, G.; Spiesz, P.; Hüsken, G.; Brouwers, H., SCC Modification by Use of Amorphous Nano-Silica. *Cem. Concr. Comp.* **2013**, *45*, 69–81. <https://doi.org/10.1016/j.cemconcomp.2013.09.001>
- (45) Xiao, M.; Xi, J.; Qiu, P.; Deng, C.; Li, F.; Wei, J.; Gao, P.; Yu, Q., Evaluation of Tensile Properties and Cracking Potential Evolution of Fly Ash-Cement Mortar at Early Age Based on Digital Image Correlation Method, *Constr. Build. Mater.* **2024**, *412*, 134855. <https://doi.org/10.1016/j.conbuildmat.2023.134855>
- (46) Shokravi, H.; Mohammadyan-Yasouj, S. E.; Rahimian Koloor, S. S.; Petru, M.; Heidarrezaei, M., Effect of Alumina Additives on Mechanical and Fresh Properties of Self-Compacting Concrete: A review, *Processes.* **2021**, *9* (3), 554 <https://doi.org/10.3390/pr9030554>
- (47) Neville, A. M.; Brooks, J. J., *Concrete Technology*, 2nd ed., Essex, England, 2010.
- (48) *Fly Ash Facts for Highway Engineers*, Technical report, American Coal Ash Association, Washington, DC, 2003.
- (49) Ulaz, B.; Turanlı, L.; Yucel, H.; Goncuoglu, M. C.; Culfaz, A., Pozzolanic Activity of Clinoptilolite: A Comparative Study with Silica Fume, Fly Ash and a Non-Zeolitic Natural Pozzolan, *Cem. Concr. Res.* **2010**, *40*, 398–404. <https://doi.org/10.1016/j.cemconres.2009.10.016>
- (50) Hossain, M.; Sultana, R.; Patwary, M.; N. Khunga, N.; Sharma, P.; Shaker, S., Self-Healing Concrete for Sustainable Buildings. A review, *Environ. Chem. Lett.* **2022**, *20*, 1265–1273. <https://doi.org/10.1007/s10311-021-01375-9>
- (51) Snoeck, D.; De Belie, N., Autogenous Healing in Strain-Hardening Cementitious Materials with and without Superabsorbent Polymers. An 8-year study, *Front. Mater.*, **2019**, *6* (48) 1–12. <https://doi.org/10.3389/fmats.2019.00048>
- (52) Cuenca, E.; Mezzena, A.; Ferrara, L., Synergy between Crystalline Admixtures and Nano-Constituents in Enhancing Autogenous Healing Capacity of Cementitious Composites under Cracking and Healing Cycles in Aggressive Waters, *Constr. Build. Mater.* **2021**, *226*, 121447. <https://doi.org/10.1016/j.conbuildmat.2020.121447>
- (53) El Fami, N.; Ez-zaki, H.; Boukhari, A.; Khachani, N.; Diouri, A., Influence of Mechanical Activation of Fly Ash on the Properties of Portland Cement Mortars, *Mater. Today: Proc.* **2022**, *58* (4) 1419–1422 <https://doi.org/10.1016/j.matpr.2022.02.340>
- (54) Zhang, W.; Zheng, Q.; Ashour, A.; Han, B., Self-Healing Cement Concrete Composites for Resilient Infrastructures: A review. *Compos. B: Eng.* **2020**, *189*, 107892. <https://doi.org/10.1016/j.compositesb.2020.107892>